BNL-66855

Tenth International Symposium on Capture Gamma Ray Spectroscopy and Related Topics (CGS10)
Santa Fe, New Mexico, August 30 -September 3, 1999

Mass Measurements Along the rp-Process Path

D. S. Brenner[1], B. E. Tomlin[1], C. E. Barton[1], N. V. Zamfir[1,2,4], R. L. Gill[3], G. Cata-Danil[2,4], R. Krücken[2], C. W. Beausang[2], R. F. Casten[2], J. Cederkall[2], Benyuan Liu[2], M. A. Caprio[2], J. R. Novak[2], J. R. Cooper[2], and Z. Wang[2]

[1]*Clark University, Worcester, Massachusetts 01610*
[2]*WNSL, Yale University, New Haven, Connecticut 06520*
[3]*Brookhaven National Laboratory, Upton, New York 11973*
[4]*Institute of Atomic Physics, Bucharest Magurele, Romania*

Abstract. The path and termination point for the rp-process above ^{56}Ni is uncertain due to a lack of knowledge of nuclear properties, especially masses, near the proton drip line. To address this need we have begun a program to measure masses of nuclei along the rp-process pathway in the A~60-80 region using β–γ coincidence spectroscopy. Results for ^{71}Se are presented and a preliminary experiment for ^{72}Br is described.

INTRODUCTION

The rapid proton-capture (rp) process, which is thought to occur in several astrophysical environments, has been proposed to account for the nucleosynthesis of proton-rich nuclei (see for example (1)). At low and moderate temperatures and matter densities in stellar environments, the termination points for the rp-process are ^{34}Ar and ^{56}Ni, respectively. At higher temperatures, characteristic of a neutron star x-ray burst, the process proceeds beyond ^{56}Ni to heavier nuclei. This is presumed to be the origin of the large solar system abundances of nuclei such as ^{92,94}Mo and ^{96,98}Ru that cannot be produced by photodisintegration of s- and r-process nuclei (2,3).

Network calculations are used to simulate the nucleosynthetic process and to model energy production in stellar scenarios. These calculations, which map reaction path and flow in this region, require considerable input data including masses, β-decay half-lives, and rates of particle-induced and photodisintegration reactions (2). Beyond Z=32 only limited amounts of experimental data are available and model calculations must be used to provide necessary input. Unfortunately, this is a region of rapidly varying nuclear structure that adds to the complexity and uncertainty of model predictions. The limitations of these input data compromise the accuracy of the rp-process calculations.

It is clear that the rp-process network calculations would benefit from experimental measurements of good precision in the region of neutron deficient isotopes beyond Z=32. Especially important is the need for nuclear mass measurements since these enter the network calculations in a variety of ways: Q_{EC} values, proton and α binding

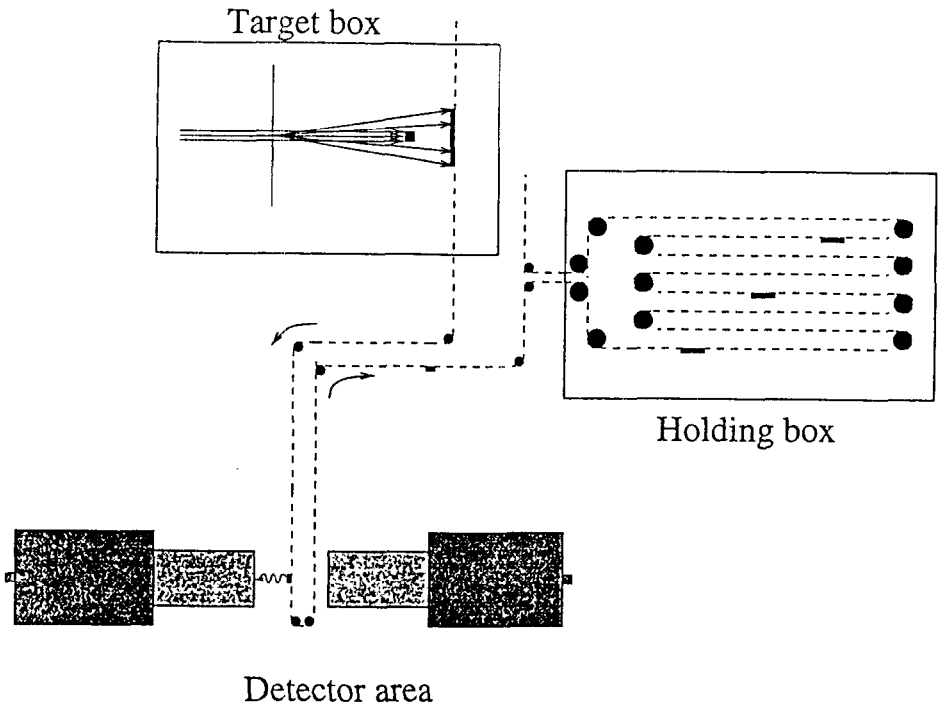

Figure 1. Schematic diagram of the apparatus used for the ^{71}Se mass measurement. See text for details.

energies. Experimental mass measurements in the rp-process region with uncertainties ≤100 keV, somewhat better than those available using mass models, could help constrain these calculations and are therefore desirable. In this paper we discuss initial experiments to measure masses of nuclei along the rp-process path using β–γ coincidence spectroscopy.

EXPERIMENTAL METHODS

We have begun a program of mass measurements using the Yale University ESTU tandem Van de Graaff accelerator. These experiments, which rely on the determination of positron spectrum end-point energies in coincidence with decay γ-rays, a conventional technique, incorporated several innovations that are described below in connection with individual experiments.

^{71}Se

We have measured the mass of the 4.74 -min ^{71}Se ground state by β–γ coincidence spectroscopy. ^{71}Se was produced by the ^{58}Ni(^{16}O,2pn) reaction. A 1 mg/cm^2 metal

foil target of ^{58}Ni, enriched to an isotopic abundance of >99%, was bombarded with a ~30-40 particle nA beam of ^{16}O ions with incident energy of 65 MeV.

A schematic drawing of the experimental apparatus is shown in Fig. 1. The target was positioned immediately behind two sets of collimators that defined a 1 mm diameter beam spot. Recoiling reaction products were collected on an aluminized Kapton tape positioned approximately 7 cm behind the target. In order to prevent the primary beam from burning the tape a 5-mm diameter Au plug was centered on the beam axis 5 cm behind target and in front of the Kapton tape. This simple arrangement resulted in the collection of ~50-70% of ^{71}Se product nuclei.

At 10-min intervals the deposit spot was moved to a shielded location where decay of the sample was measured using a Ge γ-ray detector (70% efficiency relative to NaI) and a cylindrical plastic scintillator β-ray detector (5.1 cm×5.1 cm diameter). The β^+ detector was positioned with its face parallel to the deposit side of the tape and viewed the activity spot through a 1 mg/cm^2 Mylar window. The γ-ray detector was positioned in 180° geometry. Both detectors were in close proximity to the activity spot. Pulse height and time data were digitized and recorded in event mode on magnetic tape for off-line analysis.

The Ge detector was calibrated using standard sources and verified by well-known γ-rays produced during the experiment. The plastic scintillator was calibrated from β^+ spectrum end-point measurements for ^{67}Ge and ^{70}As produced under nearly identical experimental conditions by bombardment of ^{58}Ni with ^{16}O ions at 75 MeV. The cali-

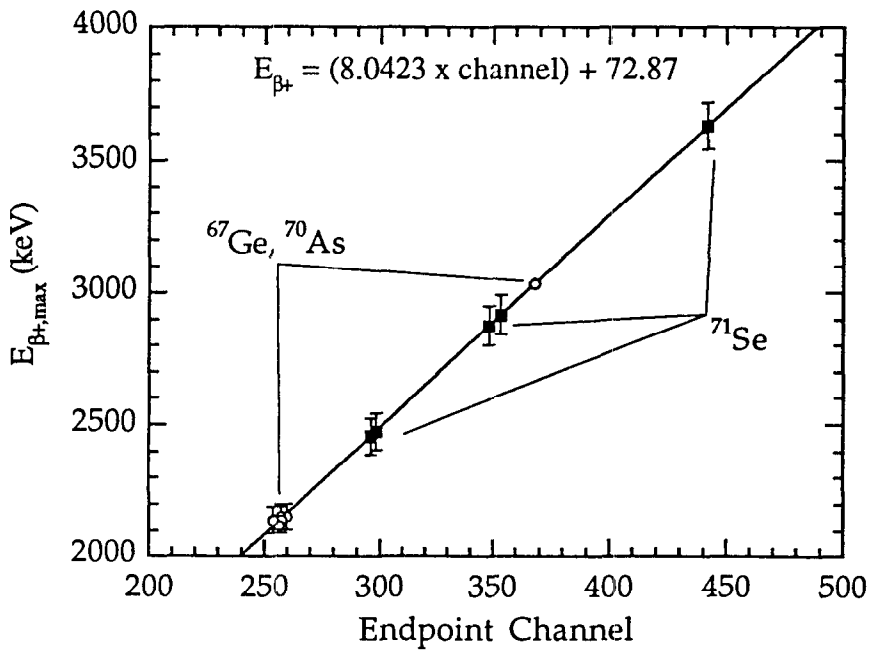

Figure 2. Calibration curve for the plastic scintillator β^+ detector determined by the end points for ^{67}Ge and ^{70}As. Also shown are the ^{71}Se end points that were used to calculate the Q_{EC} value. The equation shown is the β^+ energy calibration in keV which is applicable to data plotted in Fig. 3.

bration curve derived from the ^{67}Ge and ^{70}As β^+ spectrum end points is shown in Fig. 2 together with data for ^{71}Se decay.

Positron spectra were generated by gating on intense γ-ray and time windows for each daughter nucleus taking care to subtract the appropriate γ-ray and time backgrounds. In order to simulate a Fermi-Kurie analysis the positive square root of the counts was plotted as a function of the energy bin. The known decay scheme was then used to guide the selection of the high-energy region of the β^+ spectrum where only a single β^+ decay branch was thought to be present. In each case the selected portion of the spectrum was quite linear and a linear least-squares fit to the data was used to determine the end-point channel.

It is well known that the determination of Q_{EC} values by measurement of β^+ spectrum end points is complicated by summing effects in the β^+ detector due to random as well as coincident radiations. The former is a function of counting rate and is not a serious problem when counting rates are low, as was the case in our experiments. Summing of coincident radiation, on the other hand, is a significant problem which can be quite complex and important, depending on the decay scheme and type of detector used for the β^+ measurements. The effects of summing in the plastic scintillator were carefully scrutinized and found to be minimal. A detailed discussion of summing effects can be found in reference (4).

An example of the end-point spectra obtained for ^{71}Se is shown in Fig. 3 for the β^+ spectrum in coincidence with a 147 keV γ-ray which de-excites a level at 147 keV in ^{71}As. The β^+ endpoint energy and Q_{EC} value for this gate and for four others are listed

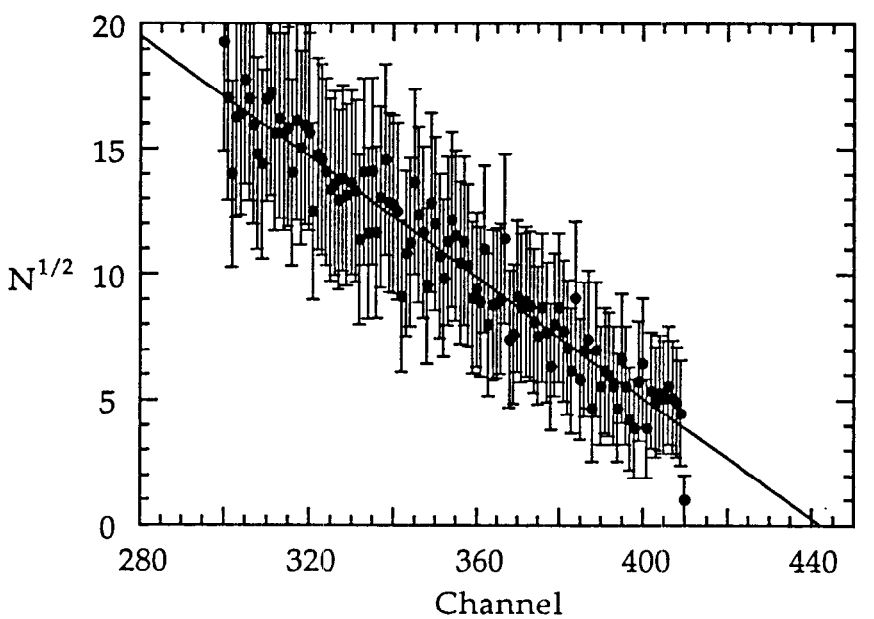

Figure 3. End-point region of the ^{71}Se β^+ spectrum gated by the 147 keV ^{71}As γ-ray.

TABLE 1. β^+ End-point Energies and Q_{EC} Values for ^{71}Se (keV).

γ-ray gate	^{71}As level energy	β^+ end-point energy	Q_{EC}
147.4	147.4	3630 (90)	4799 (90)
722.9	870.3	2875 (75)	4767 (75)
870.3	870.3	2915 (75)	4808 (75)
1095.3	1242.6	2455 (70)	4720 (70)
1242.6	1242.6	2473 (70)	4738 (70)
		(weighted mean)	4762 (35)

in Table 1. The weighted mean value for Q_{EC} is 4762(35) keV. A mass excess value of -63130(35) keV results from combing Q_{EC} with the adopted mass excess (5) of its daughter, ^{71}As. Our ^{71}Se mass excess is consistent with, but more precise than, the recently published experimental mass value of Chartier *et al.* (6) and one extrapolated from systematic trends by Audi *et al.* (5) as seen in Table 2.

^{72}Br

In some respects measuring Q_{EC} for ^{71}Se was an easy experiment since the production cross section was large, ~150 mb for the reaction chosen, and there were several strong β^+ branches to levels in the daughter nucleus ^{71}As, including one to a very low lying level at 147 keV. As one moves further from stability experiments become increasingly difficult; production cross sections drop, Q_{EC} increases on average, half lives shorten, and β^+ decay strength is spread over more levels at higher excitation energies in the daughter.

^{72}Br, our next candidate for study, illustrates some of these challenges since Q_{EC} is estimated to be ~8700 keV (7) and the production cross section is lower. In order to address these we have made several modifications to our apparatus. The tape travel distance between the target and detector station was shortened permitting us to extend

TABLE 2. Mass Excess Values for ^{71}Se (keV).

This work	Chartier *et al.*[a]	Nubase[b]
-63130 (35)	-63490 (320)	-63090 (200)

[a] Reference (6). The authors reported their uncertainties as ±250 (systematic) ±200 (statistical) which we have added in quadrature to give ±320 keV.
[b] Reference (5). Values and uncertainties are estimated from systematic trends.

studies to half-lives as short as ~1 s. In addition, in order to improve our γ-ray detection efficiency and selectivity, we replaced the single Ge detector used in the ^{71}Se experiment with three state-of-the-art Compton-suppressed Ge clover detectors arranged in an irregular geometry close to the activity spot.

To evaluate the new configuration we have done a preliminary experiment in which ^{72}Br was produced by the ^{58}Ni(^{16}O,pn) reaction. At a bombarding energy of 50 MeV the cross section for production of 78.6 s ^{72}Br is ~75mb. Although the data obtained in this run did not permit us to determine a Q_{EC} value several conclusions were evident. First, it was clear that sufficient data can be obtained with the new configuration for nuclides produced with cross sections as low as ~25 mb and half-lives as short as ~ 1 s. Second, Compton-suppressed clover γ-ray detectors have distinct advantages over conventional detectors because of their enhanced peak-to-Compton ratio and greater efficiency. We expect to have a production run on ^{72}Br in the very near future.

CONCLUSIONS

We have used a classic technique, β-γ coincidence spectroscopy, to measure the Q_{EC} value for ^{71}Se with very good precision. Introduction of modern, high-efficiency γ-ray detectors has improved the sensitivity and selectivity of the instrumentation and should permit measurements for selected nuclides in the vicinity of the rp-process path. These experiments should be feasible if the nuclide of interest has a half-life of ≥ 1 s and is produced with a cross section of ≥25 mb. The latter requirement is, of course, primarily limited by the availability of appropriate target-ion beam combinations.

In the future we plan to measure the Q_{EC} values for ^{73}Br, ^{70}Se, ^{68}As and other nuclei in the rp-process region.

ACKNOWLEDGMENTS

The U.S. Department of Energy supported this work under research grants DE-FG02-88ER40417, DE-FG02-91ER40609, and DE-AC02-98CH10886. The Clark University authors wish to express their gratitude for the hospitality and assistance provided by the staff of the Wright Nuclear Structure Laboratory, Yale University. We also wish to thank John Greene of Argonne National Laboratory for fabrication of the ^{58}Ni target.

REFERENCES

1. Lambert, D. L. *Astron. Astrophys. Rev.* **3**, 201-256 (1992).
2. Schatz, H., Aprahamian, A., Görres, J., Wiescher, M., Rauscher, T., Rembges, J. F., Thielemann, F.-K., Pfeiffer, B., Möller, P., Kratz, K.-L., Herndl, H., Brown, B. A., Rebel, H., *Phys. Rep.* **294**, 167-263 (1998).

3. Wiescher, M., Aprahamian, A., Döring, J., Görres, J., and Schatz, H., *ENAM98: Exotic Nuclei and Atomic Masses*, Sherrill, B. M., Morrissey, D. J., and Davids, C. N., eds., New York, American Institute of Physics, 1998, pp. 819-826.
4. Foy, B. D., Brenner, D. S., Davids, C. N., Seweryniak, D., Blumenthal, D., Gill, R. L., Zamfir, N. V., Warner, D. D., and Barton, C.J., *Phys. Rev. C* **58**, 749-753 (1998).
5. Audi, G., Bersillor, O., Blachot, J., and Wapstra, A. H., *Nucl. Phys.* **A624**, 1-124 (1997).
6. Chartier, M., Mittig, W., Orr, N. A., Angélique, J.-C., Audi, G., Casandijian, J.-M, Cunsolo, A., Donzaud, C., Foti, A., Lépine-Szily, A., Lewitowicz, M., Lukyanov, S., MacCormick, M., Morrissey, D. J., Ostrowski, A. N., Sherrill, B. M., Stephan, C., Suomijärvi, T., Tassan-Got, L., Vieira, D. J., Villari, A. C. C., and Wouters, J. M., *Nucl. Phys.* **A637**, 3-14 (1998).
7. Firestone, R. B., Shirley, V. S., Baglin, C. M., Chu, S. Y. F., and Zipkin, J., *Table of Isotopes*, 8th ed., New York: Wiley, p. 361.